Thermodynamics, Morphology, and Structure of the Poly(vinylidene fluoride)−Ethyl Acetoacetate System

D. Dasgupta,[†] S. Malik,[‡] A. Thierry,[‡] J. M. Guenet,*[,‡] and A. K. Nandi*[,†]

Polymer Science Unit, Indian Association for the Cultivation of Science, Jadavpur, Calcutta 700032, India, and Institut Charles Sadron, CNRS UPR 22, BP 40016, 6 rue Boussingault, F-67083 Strasbourg Cedex, France

Received May 16, 2006; Revised Manuscript Received June 24, 2006

ABSTRACT: The poly(vinylidene fluoride) (PVF_2)−ethyl acetoacetate (EAA) system produces polymer−solvent compounds. The temperature−concentration phase diagram and the Tamman's diagram indicate that the polymer−solvent complexes are of two different types which are stable in different temperature regions; one is a congruently melting compound while the other is of the singular type. Also, a metatectic-like behavior is observed due to the peculiar melting behavior of PVF_2. The morphology of the compounds resembles a "crumpled cloth" network, with the probable presence of chain-folded lamellae. SAXS study indicates presence of chain-folded lamellae of lamellar thickness 8 nm in the PVF_2−EAA systems. FTIR and WAXS spectra indicate formation of α polymorphic structure of PVF_2, and they are consistent with the occurrence of compounds. Indeed, two new X-ray diffraction peaks are observed for the system at $2\theta = 22.2°$ and 24.0° near the polymer−solvent complex stoichiometric composition ($W_{PVF_2} = 0.33$). The FTIR spectrum also shows a new peak at 592 cm^{-1} for the complex formation at the stoichiometric composition. Molecular modeling using the MMX program supports the polymer−solvent complexation in this system.

Introduction

Poly(vinylidene fluoride) (PVF_2) is a technologically important polymer. In the solid state it exhibits five different polymorphic structures, of which the β-polymorph is piezoelectric in nature.[1] It produces thermoreversible gels in organic diesters, yet the gel morphology depends on the number of intermittent carbon atoms (n) present in the diesters.[2] The fibrillar morphology has been attributed to the formation of polymer−solvent complexes, which are better enthalpically and entropically stabilized with increasing intermittent carbon atoms.[2] Ethyl acetoacetate (EAA) has a chemical structure very similar to that of diethyl malonate ($n = 1$), and the keto carbonyl group is more polar than the ester carbonyl group. As a result, there is a high probability for establishing a strong specific interaction between the ⟩C═O group of EAA and ⟩CF_2 groups of PVF_2.[3,4] Thus, there is a possibility of polymer−solvent complex formation in this system. In this paper we report on the morphology, the structure, and the thermodynamics of the PVF_2−ethyl acetoacetate (EAA) system.

Thermoreversible polymer gels have been studied extensively for the past two decades.[5−7] By proper drying these gels can be easily transformed into multiporous materials.[8,9] The thermoreversible gels usually have a three-dimensional network structure which are reversibly formed and destroyed during cooling and heating processes.[10−14] In some cases, these gels are produced thanks to the formation of polymer−solvent compounds.[6] This is because on cooling polymer−solvent complexes are produced and on heating they usually break.[2] Polymer−solvent compound formation is usually observed from thermodynamic investigations, namely temperature−concentration phase diagrams,[11,15] X-ray diffraction,[16] neutron diffraction,[17,18] NMR,[19] and FT-IR spectroscopy.[2,11] Here PVF_2−EAA complexation has been investigated by mapping out the temperature−concentration phase diagram[20] and by performing X-ray and FT-IR spectroscopy experiments. Finally, the polymer−solvent complexation in this system is evaluated from molecular modeling using the MMX program.[21]

* Corresponding authors: E-mail: guenet@ics.u-strasbg.fr; psuakn@mahendra.iacs.res.in.
[†] Indian Association for the Cultivation of Science.
[‡] CNRS UPR 22.

Experimental Section

Samples. Poly(vinylidene fluoride) (PVF_2) is a product of Aldrich Chemical Co. The weight-average molecular weight ($\bar{M}_w$) of the sample is 1.8×10^5, and the polydispersity index is 2.54 as supplied by the company. The PVF_2 sample was recrystallized from its 0.2% (w/v) solution in acetophenone. Ethyl acetoacetate was purchased from Spectrochem Pvt Ltd. (Bombay, India) and was distilled under reduced pressure before use.

Sample Preparation and Characterization. The required amounts of PVF_2 and EAA were taken in a thick-walled glass tube (8 mm in diameter and 1 mm thick) and degassed by repeated freeze−thaw technique, and the tubes were sealed. The samples in sealed tubes were melted at 210 °C in an oven for 20 min with intermittent shaking to make it homogeneous. They were then quenched to room temperature (30 °C).

For SEM study the sample was taken out by breaking the tube and was dried by exposing it at room temperature for 2 days and finally dried in a vacuum at 40 °C for 5 days. It was then coated with a gold layer of thickness 40 nm by the sputtering technique in an argon atmosphere and was then observed in a SEM apparatus (Hitachi S-2300). The FT-IR study was carried out using a Nicolet FT-IR instrument (Magna IR 750 spectrometer, series II). The sample spectrum was then subtracted from the EAA spectrum using Omnic software (version 3.1) to obtain the PVF_2 spectra in the pure state.

Thermal Characterization. For thermodynamic study the samples of different compositions were prepared in Perkin-Elmer large volume capsules (LVC) by taking appropriate amounts of polymer and solvent, and the capsules were tightly sealed with the help of a quick press. They were subsequently made homogeneous by keeping at 210 °C in DSC (DSC-7, Perkin-Elmer) for 20 min. They were cooled at a rate of 200 °C/min to −30 °C and were kept at −30 °C for 10 min. They were then heated at the scan rate

10.1021/ma0610921 CCC: $33.50
Published on Web 07/29/2006

of 10°/min under a nitrogen atmosphere from −30 to 210 °C. The enthalpy(s) and melting temperature(s) were measured with the help of a computer attached to the instrument using PC series DSC-7 multitasking software (Version 3.2). The instrument was calibrated with cyclohexane and indium before each set of experiment. Some experiments were also performed by making the samples outside in a glass tube and then putting it in aluminum pans, which were then hermetically sealed. The results obtained in the two methods were found to be consistent for the same composition of the system.

WAXS Investigation. The WAXS experiments were carried out on the PVF_2−EAA systems at 30 °C. The experiment was performed in a Seifert X-ray diffractometer (C3000) with nickel-filtered copper Kα radiation equipped with a parallel beam optics attachment. The instrument was operated at a 35 *k*V voltage and a 30 mA current and was calibrated with a standard silicon sample. The samples were placed on aluminum holder and were scanned from a $2\theta = 10°$ value at the step scan mode (step size 0.03°, preset time 2 s), and the diffraction pattern was recorded using a scintillation counter detector.

SAXS Study. The temperature-dependent small-angle X-ray (SAXS) experiments of the PVF_2−EAA system were carried out on beamline BM2 at the European Synchrotron Radiation Facility (ESRF), Grenoble, France. The energy of the beam was 15.8 keV, which corresponds to a wavelength of $\lambda = 7.86 \times 10^{-2}$ nm. The collimated beam was focused with a typical cross section of 0.1 × 0.3 mm^2. The scattered radiation was collected onto a two-dimensional CCD detector developed by Princeton Instruments. Data acquisition times are of about 10−20 s, which allows time-resolved experiments to be carried out at 2 °C/min.

The sample-to-detector distance was set at 1.48 m, which corresponds to a momentum transfer vector q range of $0.1 < q\ (nm^{-1}) < 3$, with $q = (4\pi/\lambda)\sin(2\theta/2)$, where λ and 2θ are the wavelength and the scattering angle, respectively. The scattered intensities were corrected for detector efficiency, dark current, empty cell scattering, sample transmission, and sample thickness. To obtain a one-dimensional X-ray pattern out of the two-dimensional digitalized pictures, the data were radially regrouped and a silver behenate sample was used for calculating the actual values of the momenta transfer q. The samples were placed in glass tubes of 3 mm diameter that were sealed to prevent from solvent evaporation. A minimum of 200 mg of material was used in order to make sure that the sample was homogeneous throughout.

Molecular Modeling. To get an approximate idea of the polymer−solvent complexes, a molecular model of the PVF_2−EAA system has been done from a PC (Pentium III) using a molecular mechanics (MMX) program.[21] The structure of the α polymorphic PVF_2 and that of EAA molecules are drawn with the help of the program such that the oxygen atom of ⟩C═O group of EAA faces the carbon atoms of the ⟩CF_2 group of PVF_2. The whole structure was then energetically minimized with the help of the MMX program, and the distances between the carbon atom of the ⟩CF_2 group and the oxygen atom of the ⟩C═O group are queried.

Results and Discussion

Thermodynamics. Typical DSC thermograms obtained from PVF_2−EAA systems display two melting endotherms as does the pure PVF_2 sample also (Figure 1). This double melting is not due to a melt-recrystallization phenomenon[22,23] as it is for pure PVF_2 sample. Figure 1 illustrates that pure PVF_2 has two melting peaks at the heating rate 10 °C/min, and at the heating rate of 40 °C/min it exhibits single melting peak (inset of Figure 1), indicating melt-recrystallization in the sample during heating. But in the PVF_2−EAA system there is no such heating rate dependency of the thermograms shape; i.e., the ratio between the two endotherms is independent of the heating rate (cf. Figure 1 and its inset). This indicates that there is no melt-recrystallization in the PVF_2−EAA system. So the peaks of the PVF_2−EAA system (Figure 1) may be considered as new and may be assigned for the polymer−solvent complexes produced

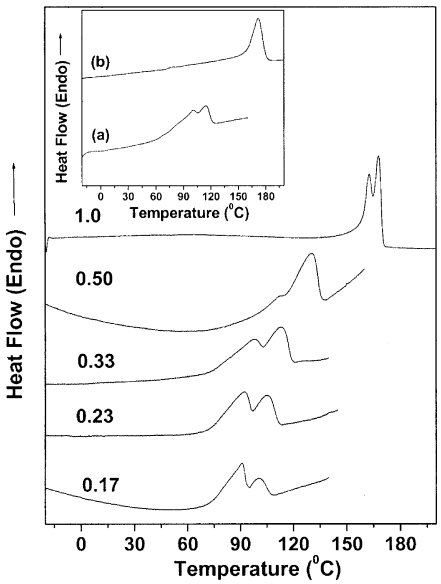

Figure 1. DSC heating thermograms of PVF_2−EAA systems at indicated polymer weight fractions at the rate 10°C/min. Inset: DSC heating thermograms of (a) PVF_2−EAA ($W_{PVF_2} = 0.33$) and (b) pure PVF_2 at the rate 40 °C/min.

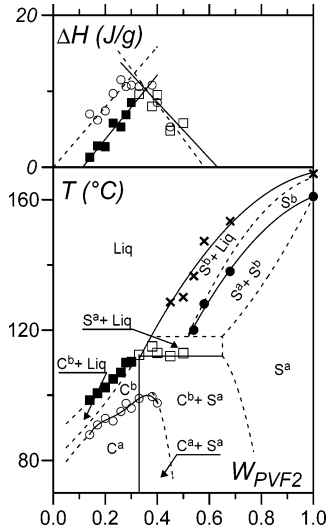

Figure 2. Temperature−concentration phase diagram for the system PVF_2−EAA. (bottom) Phase diagram: ○, melting peak of C^a (1st endotherm); ■, melting peak of C^b (2nd endotherm); □, melting of C^b indicating nonvarient region; ●, melting peak of S^a (i.e., lower melting PVF_2); ×, melting peak of S^b (i.e., higher melting PVF_2). (top) Tamman's diagram: The symbols used for the data in the Tamman's diagram (melting enthalpies vs concentration in the upper diagram) correspond to the thermal events in the *T,C* phase diagram. As explained in the text, the dotted lines are deduced on the basis of Gibbs phase rules.

in the system discussed below. In fact, for pure PVF_2 two types of lamellae are dealt with, hence the double melting. The melting temperatures are reported in the temperature−concentration phase diagram plotted in Figure 2. This figure reveals interesting features. A nonvariant event can be observed at $T = 113 \pm 2$ °C (nonvariant event = temperature associated with an endotherm is a constant with increasing polymer concentration). It corresponds to a sharp rise in the melting temperature associated with the first endotherm. The Tamman's diagram (namely the various latent heats plotted as a function of polymer concentration) plotted in the same figure shows that the enthalpy (latent heat) associated with the low-melting endotherm goes through a maximum at a concentration $W_{PVF_2} = 0.31$ w/w. Also, the

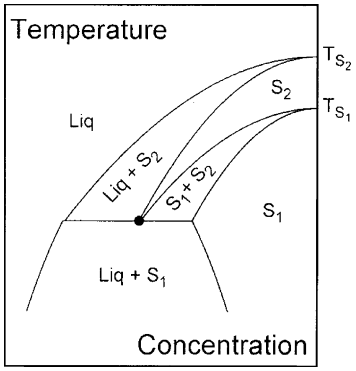

Figure 3. A typical metatectic transition. Here the solid displays two stable crystalline forms. At T_{S_1} form I transforms into form II while at T_{S_2} form II melts. Adding a solvent produces a metatectic transition where S_1 + liq ⇒ S_2 at the *metatectic* point (●).

enthalpies associated with the high-melting endotherm and the nonvariant endotherm cross at a concentration $W_{PVF_2} = 0.35$ w/w. These observations suggest the existence of a polymer−solvent compound whose stoichiometric concentration is $W_{PVF_2} = 0.33 \pm 0.02$ w/w. This corresponds to a stoichiometry of approximately one solvent molecule per monomeric unit of PVF_2.

To draw a phase diagram consistent with Gibbs phase rules, we have to consider a metatectic-like transition. Such a transition occurs when a solid can display two stable crystalline forms in the bulk state. At a given temperature one form transforms into the other, while releasing latent heat. As a result, two endotherms are observed: the first endotherm is related to the transition from one crystalline form into the other, and the last endotherm is due to the melting of the stablest form. When a binary system is studied, such as polymer + solvent, this gives rise to a so-called metatectic transition (see Figure 3). Here, a strong resemblance with such a transformation is seen due to the fact that pure PVF_2 also displays two melting endotherms, although their origin are not due to a transformation from one form to the other. The phase diagram can, however, be drawn by using the procedure that would be applied for a metatectic transformation. Such an approach was already taken for the system PVF_2−camphor in a previous publication.[16]

The complete phase diagram is mapped out in Figure 2 by applying Gibbs phase rules, particularly by fulfilling the number of phases as derived from the relation between the variance of a system and the number of constituents.[19,20] This relation states that for a two-component system at constant pressure *T*,*C* domains cannot contain more than two phases, and not more than three phases can coexist at a given *T*,*C* coordinate. Dotted lines stand for probable extrapolation again on the basis of phase rules.

The phase diagram shows that compound C^a leaves compound C^b when melting, whose stoichiometries are the same, and most probably the crystal structure is identical or nearly identical. Similarly, two solid phases, S^a and S^b, are present. From this phase diagram, we infer that C^b is probably of the "singular point" type of compound (namely, the limiting case between a congruently melting compound and an incongruently melting compound). The temperature nonvariant event is therefore the transformation of C^b into a solid phase S^a. Conversely, C^a is likely to be a congruently melting compound.

Morphology. Figure 4a,b shows the SEM micrographs of the dried samples of compositions $W_{PVF_2} = 0.17$ and 0.30 of PVF_2−EAA systems where compound C^a is produced at room temperature. After the removal of solvent "crumpled cloth"

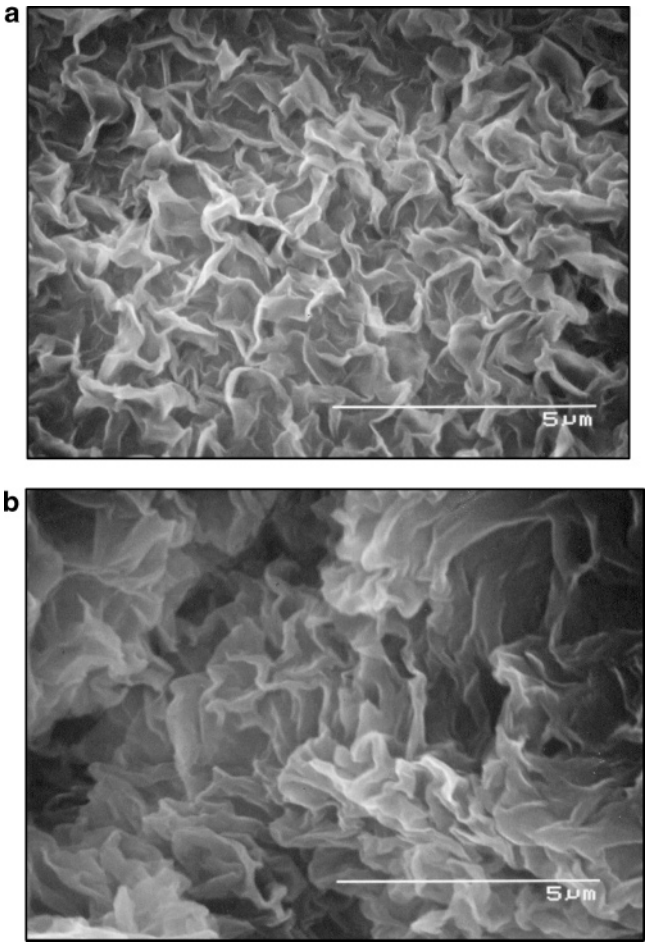

Figure 4. Scanning electron micrographs of the PVF_2−EAA system **(a)** ($W_{PVF_2} = 0.17$) and **(b)** ($W_{PVF_2} = 0.30$).

morphology is observed in both the cases. The average thickness of the sheets are found to be 84 and 132 nm for samples of compositions $W_{PVF_2} = 0.17$ and 0.30, respectively. The average long period of the sample of composition $W_{PVF_2} = 0.30$ was measured from temperature-dependent small angle X-ray scattering using synchrotron radiation source at Grenoble, and its value is 16.1 nm (Figure 5). Generally, PVF_2 is 50% crystalline[1] so the average lamellar thickness is 8.05 nm.

Thus, it may be surmised that the "crumpled cloth" morphology may arise from the stacking of 10 and 16 chain-folded lamella of PVF_2 for the compositions $W_{PVF_2} = 0.17$ and 0.30, respectively. So in this system polymer−solvent complexation does not prevent chain folding completely, and chain-folded lamella stacked to form "crumpled cloth" morphology. This morphology is different from the fibrillar morphology obtained in the diesters.[2] In Figure 5 it is apparent from the temperature-dependent SAXS data that the lamella peak almost vanishes at 127 °C for the composition $W_{PVF_2} = 0.30$. The DSC melting peak temperature of higher melting endotherm is 112 °C while its end temperature is 118 °C, which approximately corresponds to the disappearance of lamellar peak. The difference, e.g. 9 °C, might arise due to the use of slower heating rate (2 °C/min) in the X-ray experiment causing thermal annealing. So the phase diagram is approximately supported by small-angle X-ray data.

Structure. The structure of the PVF_2−EAA system has been determined from WAXS pattern and FT-IR spectroscopy. In Figure 6 the FT-IR spectra of pure components, the PVF_2−EAA system ($W_{PVF_2} = 0.33$) and the solvent-subtracted FT-IR spectra of PVF_2−EAA system ($W_{PVF_2} = 0.33$) are presented. In the PVF_2−EAA system there is a new peak at 592 cm^{-1}

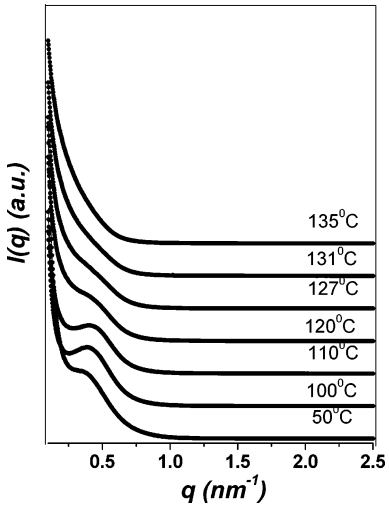

Figure 5. Temperature-dependent small-angle X-ray diffractograms of the PVF_2−EAA system ($W_{PVF_2} = 0.30$) at indicated temperatures.

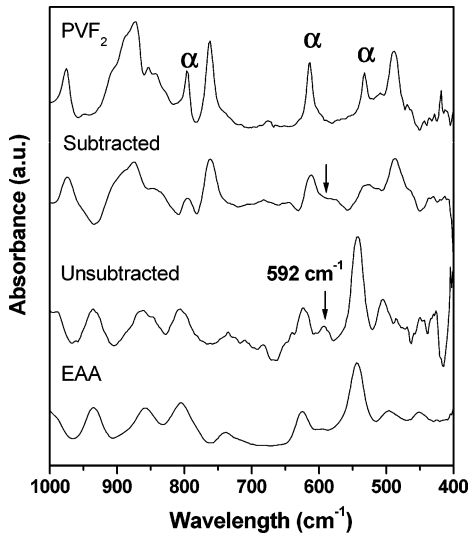

Figure 6. FT-IR spectra of the PVF_2−EAA system ($W_{PVF_2} = 0.33$), pure PVF_2, EAA, and solvent-subtracted spectrum of the PVF_2−EAA system ($W_{PVF_2} = 0.33$).

that may be attributed to polymer−solvent complexation. In the solvent-subtracted spectrum, the peak is transformed into a hump complying with the polymer−solvent compound formation. From the solvent-subtracted spectra it is also clear that there are peaks at 794, 613, and 532 cm^{-1} characterizing the formation of α polymorph PVF_2 in the PVF_2−EAA system.[24−26] Figure 7 illustrates the WAXS patterns of the PVF_2−EAA system at compositions $W_{PVF_2} = 0.21$, 0.33, and 0.40, and it shows the characteristic diffraction peaks of α-polymorph PVF_2 at $2\theta =$

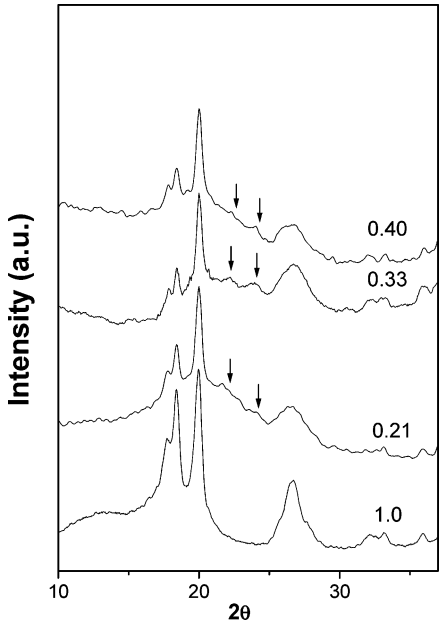

Figure 7. WAXS pattern of PVF_2−EAA systems of compositions $W_{PVF_2} = 0.21$, 0.33, and 0.40 along with that of melt-crystallized PVF_2 (1.0).

17.7°, 18.4°, 20.0°, 26.6°, and 38.6°.[27−30] At the complex stoichiometric composition ($W_{PVF_2} = 0.33$) two new diffraction peaks appear at $2\theta = 22.2°$ and 24.0° that can be attributed to polymer−solvent complexation. Interestingly, these peaks are not so intense for the samples of compositions $W_{PVF_2} = 0.21$ and 0.40 as they rather appear as shoulders. This is consistent with the phase diagram which indicates that the maximum amount of complex is obtained for $W_{PVF_2} = 0.33$ and that below and above this concentration the fraction of complex decreases. The d_{hkl} values and the intensity ratio (I^0_{hkl}/I^0_{110}) of the system are also compared with the melt-crystallized PVF_2 sample in Table 1. It is apparent from the table that the intensity ratio values of the samples do not exactly match with those of the melt crystal.[27,28] In the powder diffraction geometry, the variations of relative intensities of a given peak are related to some local disorder or orientation of the sample. Thus, although the *d* spacings of the main peaks of the sample remain the same with those of melt crystal, the atomic positions of the statistical up and down arrangement of the chains may be somewhat changed due to the polymer−solvent complex formation. It is also evident from the table that the deviation of relative intensities in the diffraction peaks is significantly higher for the sample with complex composition ($W_{PVF_2} = 0.33$). Therefore, both the presence of new diffraction peaks and the variation in intensity ratio clearly support the formation of polymer−solvent complex in this system.

Table 1. WAXS Data of PVF_2−EAA Systems[a]

hkl	(d_{hkl}) calcd (Å)	(d_{hkl}) obsd (Å)	I^0_{hkl}/I^0_{110} melt cryst	PVF_2−EAA $W_{PVF_2} = 0.21$, I^0_{hkl}/I^0_{110}	PVF_2−EAA $W_{PVF_2} = 0.33$, I^0_{hkl}/I^0_{110}	PVF_2−EAA $W_{PVF_2} = 0.40$, I^0_{hkl}/I^0_{110}
100	5.00	5.00	0.68	0.64	0.58	0.66
020	4.81	4.82	0.92	0.75	0.67	0.74
110	4.44	4.44	1.00	1.00	1.00	1.00
		4.0		0.59	0.63	0.54
		3.69		0.47	0.61	0.48
021/101	3.33	3.34	0.48	0.49	0.69	0.48
121	2.79	2.79	0.24	0.32	0.54	0.35
130	2.7	2.70	0.25	0.33	0.54	0.36
200	2.49	2.5	0.24	0.32	0.60	0.38

[a] d_{hkl} calculated for α-phase of PVF_2 with $a = 5.02$ Å, $b = 9.63$ Å, and $c = 4.62$ Å; I^0_{hkl} = observed intensity.

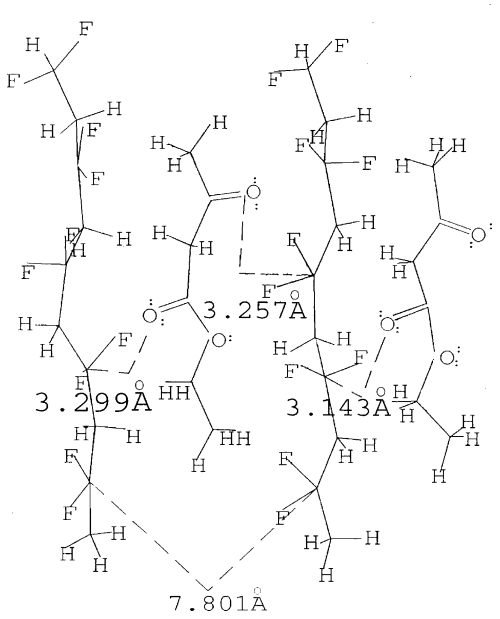

Figure 8. An approximate molecular model of the PVF_2−EAA complex of composition PVF_2 monomer:EAA = 1:1 drawn from the MMX program.

Molecular Modeling. An approximate structure of PVF_2−EAA complex (Figure 8) has been built up by molecular mechanics calculation using MMX program. EAA molecules are placed by the side of PVF_2 chain (α phase) in a way that the ⟩C═O group of EAA molecule faces the ⟩CF_2 group of PVF_2 as there is some dipolar interaction between these two groups.[3,4] The two ⟩C═O groups of an EAA molecule face two ⟩CF_2 groups of two PVF_2 chains producing an intermolecular complex. The whole structure was then energetically minimized with the help of the program, and the distances between the carbon atom of the ⟩CF_2 group and oxygen atom of carbonyl group are queried. The values are found to be 3.14, 3.25, and 3.29 Å. The van der Waals radius of the ⟩CF_2 group is 2.25 Å and that of oxygen is 1.40 Å, yielding distance for interatomic contact to be 3.65 Å.[2,31] Here all the queried distances have values less than 3.65 Å, indicating the presence of dipolar interaction between ⟩CF_2 and ⟩C═O groups in the system. This interaction primarily supports the formation of polymer−solvent complex in the system. The distance between the PVF_2 strands is 7.8 Å, indicating that micropores may be created after careful drying of the system apart from the macrosized pores arising from solvent entrapment by the PVF_2 stacked lamella as shown in Figure 4a,b.[9]

Conclusion

The PVF_2−EAA system exhibits "crumpled cloth" network morphology formed from stacked PVF_2 lamella. The phase diagram and Tamman's plot of the PVF_2−EAA system indicate polymer−solvent complexation with two different complexes of same stoichiometric composition stabilized in different temperature region. This is due to the peculiar melting behavior of pure PVF_2, which exhibits two melting endotherms that are related to melt-recrystallization phenomenon. In particular, the phase diagram is interpreted by contemplating a metatectic-like transition. WAXS and FT-IR spectra suggest the formation of α polymorphic PVF_2. New diffraction peaks at $2\theta = 22.2°$ and 24.0° in WAXS spectra and a new peak at 592 cm^{-1} in the FT-IR spectra may be attributed for the formation of polymer−solvent complexes in the PVF_2−EAA system. SAXS study indicates the presence of chain-folded lamella of thickness ∼8 nm, whereas the stacked lamella have thickness 84 and 132 nm for the composition $W_{PVF_2} = 0.17$ and 0.30, respectively. This indicates stacks of 10 and 16 lamella produce the "crumpled cloth" morphology of $W_{PVF_2} = 0.17$ and 0.30, respectively. An approximate molecular model using the MMX program also supports polymer−solvent complexation in the system.

Acknowledgment. We gratefully acknowledge the Indo-French Center for the Promotion of Advanced Research (IFCPAR, Grant No. 2808-2) for financial support.

References and Notes

(1) Lovinger, A. J. In *Developments in Crystalline Polymers, 1*; Basset, D. C., Ed.; Elsevier Applied Science: London, 1981; p 195.
(2) Dikshit, A. K.; Nandi, A. K. *Macromolecules* **2000**, *33*, 2616.
(3) Roerdink, E.; Challa, G. *Polymer* **1980**, *21*, 509.
(4) Belke, R. E.; Cabasso, I. *Polymer* **1988**, *29*, 1831.
(5) *Reversible Polymeric Gels and Related Systems*; Russo, P. S., Ed.; American Chemical Society: Washington, DC, 1987.
(6) Guenet, J. M. *Thermoreversible Gelation of Polymers and Biopolymers*; Academic Press: London, 1992.
(7) Nijenhuis, K. te. *Adv. Polym. Sci.* **1997**, *130*, 1.
(8) Guenet, J. M.; Ray, B.; Elhasri, S.; Marie, P.; Thierry, A. *NATO Sci. Ser. 1V: Earth Environ. Sci.* **2003**, *24*, 191.
(9) Dasgupta, D.; Nandi, A. K. *Macromolecules* **2005**, *38*, 6504.
(10) Mal, S.; Nandi, A. K. *Polymer* **1998**, *39*, 6301.
(11) Dikshit, A. K.; Nandi, A. K. *Macromolecules* **1998**, *31*, 8886.
(12) Berghmans, M.; Thijs, S.; Cornette, M.; Berghmans, H.; De Schyver, P. C.; Moldenaers, P.; Mewis, J. *Macromolecules* **1994**, *27*, 7669.
(13) Guenet, J. M.; McKenna, G. B. *Macromolecules* **1988**, *21*, 1752.
(14) Guenet, J. M. *J. Rheol.* **2000**, *44*, 947.
(15) Mal, S.; Nandi, A. K. *Langmuir* **1998**, *14*, 2238.
(16) Dasgupta, D.; Manna, S.; Malik, S.; Rochas, C.; Guenet, J. M.; Nandi, A. K. *Macromolecules* **2005**, *38*, 5602.
(17) Guenet, J. M. *Macromolecules* **1987**, *20*, 2874.
(18) Saiani, A.; Spevacek, J.; Guenet, J. M. *Macromolecules* **1998**, *31*, 703.
(19) Spevacek, J.; Suchoparek, M. *Macromolecules* **1997**, *30*, 2178.
(20) Guenet, J. M. *Thermochem. Acta* **1996**, *284*, 67.
(21) Gajewski, K. E.; Gillberr, M. H. In *Advances in Molecular Modeling*; Liotta, D., Ed.; Jai Press: Greenwich, CT, 1990; Vol. 2.
(22) Prest, W. M., Jr.; Luca, D. J. *J. Appl. Phys.* **1975**, *46*, 4136.
(23) Nandi, A. K.; Mandelkern, L. *J. Polym. Sci., Part B: Polym. Phys.* **1991**, *29*, 1287.
(24) Cortilli, G.; Zebri, G. *Spectrochem. Acta* **1967**, *23A*, 2218.
(25) Tashiro, K.; Kobayashi, M. *Phase Transitions* **1989**, *18*, 213.
(26) Kobayashi, M.; Tashiro, K.; Tadokaro, H. *Macromolecules* **1975**, *8*, 158.
(27) Lando, J. B.; Doll, W. W. *J. Macromol Sci., Phys.* **1968**, *2*, 205.
(28) Hasegawa, R.; Takahashi, Y.; Chatani, Y. *Polym. J.* **1972**, *3*, 600.
(29) Bachmann, M. A.; Lando, J. B. *Macromolecules* **1981**, *14*, 40.
(30) Datta, J.; Nandi, A. K. *Polymer* **1997**, *38*, 2719.
(31) Pauling, L. *The Nature of Chemical Bond and the Structure of Molecules and Crystals*, 3rd ed; Cornell university Press: Ithaca, NY, 1960; p 227.

MA0610921